Publié dans : Journal of Performance of Constructed Facilities, Vol. 31, Issue 3 (Octobre 2016) https://doi.org/10.1061/(ASCE)CF.1943-5509.0000960

Methods for shear strengthening of thick concrete slabs

Mathieu Fiset[1], Josée Bastien[2] and Denis Mitchell[3]

Abstract:

This paper presents different strengthening techniques to improve the shear capacity of existing thick concrete slab structures that were constructed without shear reinforcement. Reinforcing bars are installed into vertical drilled holes and anchored with epoxy adhesive to increase the shear capacity. Experiments on retrofitted beams, representing slab strips, showed that all of the strengthening techniques investigated resulted in increased shear capacities. The shear failure mechanisms of the strengthened beams showed that, as expected, current evaluation methods for elements with conventional, well-anchored stirrups can lead to an overestimation of the shear capacities. The efficiency of the strengthening techniques is strongly influenced by the performance of the end anchorage of the drilled-in bars. The effectiveness of the epoxy-bonded bars is a function of their embedded length and they can, in some cases, debond before they reach their yield strength. By using the maximum bar spacing required by the Canadian Highway Bridge Design Code or the AASHTO-LRFD design specifications, bonded shear reinforcing bars may debond and offer poor performance. A maximum transverse reinforcement spacing criterion is therefore suggested for the added bonded bars.

[1] Ph. D. Candidate, Research Center on Concrete Infrastructures, Dept. of Civil Engineering, Université Laval., Quebec city, QC, Canada, G1V 0A6 (Corresponding author). E-mail: Mathieu.Fiset.1@ulaval.ca
[2] Professor, Research Center on Concrete Infrastructures, Dept. of Civil Engineering, Université Laval., Quebec city, QC, Canada, G1V 0A6. E-mail: Josee.Bastien@gci.ulaval.ca
3 Professor, Dept. of Civil Engineering and Applied Mechanics, McGill University. Montréal, QC, Canada. E-mail: Denis.Mitchell@mcgill.ca

Introduction

Concrete thick slab bridges typically have spans ranging from 6 m to 25 m (20’ to 80’) with a structural slab thickness of 300 mm to 1500 mm (12 in. to 60”). For this simple structural system, the thick slab is designed to carry all loads and therefore no support beams (girders) are required. For the design of thick concrete slabs, it is often assumed that the shear capacity provided by the concrete is sufficient to resist the shear and therefore, no shear reinforcement is required. On September 30th, 2006, the Concorde overpass (Laval, Quebec, Canada) collapsed, killing five people and injuring six others (Fig. 1). Even though the original design complied with standards at the time of construction, a shear failure in the cantilever region of the supporting concrete thick slab led to collapse (Johnson et al. 2007; Mitchell et al. 2011). This shear failure occurred in the 1200 mm (48 in.) thick slab that did not contain any shear reinforcement. The shear failure was very brittle and lead to the sudden collapse of one-half of the overpass structure. For the Concorde overpass collapse, the investigation has shown that concrete degradation with time resulted in the propagation of inclined cracks, followed by a brittle shear failure. That tragic event raised questions concerning the safety of many aging thick concrete slab bridges without shear reinforcement. Moreover, the investigation showed that the provision of the minimum amount of shear reinforcement recommended by the 2014 Canadian Highway Bridge Design Code S6 (CHBDC) (CSA 2014a) would have prevented the Concorde overpass collapse. Because of the deficiencies in shear of this type of construction, practical methods incorporating shear reinforcing bars into thick concrete slabs have gained wide interest.

Some shear strengthening methods have already been studied on narrow beams. The addition of near surface mounted rods (De Lorenzis and Nanni 2001; Dias and Barros 2008) and the addition of external carbon fiber reinforced plastic (FRP) laminates (Adhikary and Mutsuyoshi 2006;

Teng et al. 2009) have been proven successful to increase shear capacity. However, the anchorage of such shear reinforcement on either side of a concrete beam section raised question of their efficiency on the full width of wide structural elements like thick slab bridges. On one hand, thin slabs strengthened in shear with bonded inclined drilled-in rods have shown their efficiency to increase punching shear capacity (Fernández Ruiz et al. 2010). On the other hand, very few studies were performed on the strengthening of existing thick slabs where the well known "size effect" (Godat et al. 2010; Collins et al. 2008) will influence the shear capacity.

This paper presents shear strengthening techniques that can be used on existing concrete thick slab structures to improve the shear capacity (Fig. 2). The loading tests performed as well as the comparison between shear capacities of concrete thick slab strips (beams) strengthened and unstrengthened in shear are presented. The techniques investigated consist of placing reinforcing bars into pre-drilled vertical holes with epoxy bonding. The performance of this system has been examined through experimental tests. The responses of the strengthened beams are compared to tested reference beams, with conventional stirrups and without stirrups.

Description of Post-Installed Shear Strengthening methods

Fig. 2 shows the installation of two strengthening techniques. The first method (Fig. 2a) consists of filling drilled holes with high-performance epoxy adhesive to bond the full length of steel bars to the concrete. For this case, the holes are drilled from the top surface and the bars are inserted into the epoxy-filled holes from the top. The alternative method (Fig. 2b) consists of introducing the epoxy-bonded shear reinforcement from both the top and bottom slab faces, in order to provide longer bar embedded lengths near the bottom surface.

Experimental Program

Two series of three point loading tests were performed for a total of 15 beams representing thick

slab strips (beams) which were designed to experience shear failures. All simply supported beams (4000 mm span) have a rectangular cross section of 610 mm width, b_w, and constant heights, h, of 450 mm or 750 mm. Details of the beams are presented in Table 1 and Fig. 3. Three reference specimens, (U1, U2, and U3), without shear reinforcement were also tested. These beams are not shown in Fig. 3 but they have the same overall dimensions and flexural reinforcement as the shear strengthened beams B1, B2 and B3.

Description of the 1st test series

Beam specimens U1, U2 and U3, and their companion beams with post-installed epoxy bonded bars B1, B2 and B3 were designed to study the effectiveness of the bonded shear reinforcement on the beam shear capacities. The spacing ratio, equal to the spacing of the bars, s_v, divided by the effective shear depth, d_v, of the post-installed shear reinforcement is close to the maximum allowed by North American Standards ($k_{v,max} = s_{v,max} / d_v$ = 0.75 and 0.80 for CHBDC S6 (CSA 2014a) and AASHTO (2012) respectively). Beams B1 and B3 were strengthened using 15M reinforcing bars whereas beam B2-1 and B2-2 were strengthened with 10M reinforcing bars (refer to Table 2 for the bar area, A_b, and the bar diameter, d_b). These post-installed bars were introduced into 14.3 and 19.1 mm diameter holes for the 10M and 15M bars, respectively, and bonded to the concrete with epoxy adhesive (Fig. 2a). The longitudinal reinforcement ratio ρ is presented in Table 1 and, for this first series of beams, 25M bars were used for longitudinal tension reinforcement.

Description of the 2nd test series

Specimens of the second series, which were all strengthened in shear, provide results to compare different reinforcing methods. Beams B4, B5 and S1 have transverse reinforcement spaced such that the ratio $k_v = s_v / d_v$ was 0.61. Beam S1 is a typical reinforced concrete beam with 15M

conventional stirrups. Beams B4 and B5 were strengthened with vertical 15M epoxy-bonded bars post-installed into 19.1 mm diameter holes. The post-installed bars in beam B4 were installed from the top face of the beam, whereas they were installed from both top and bottom faces for beam B5 (Fig. 3b). For this series, 30M bars were used for longitudinal tension reinforcement in the beams.

Material Properties

The average compressive strengths of the concrete, $f_c^{'}$, presented in Table 1 were determined at an age at which the beams were tested. The maximum aggregate size of the concrete, a_g, was 19 mm for all specimens and the concrete density, γ_c, is presented in Table 1. The steel reinforcing bars yielding strength, f_y, and ultimate strength, f_u, are given in Table 2. For all bars, the Young modulus, E_s, was taken as 200 GPa. A commercially available epoxy adhesive was used for the bonded anchorage. The bond strength, τ_b, of the epoxy adhesive was estimated as (Fernández Ruiz et al 2010, ETA 2013):

$$\tau_b = 18.7\left(\frac{f_c^{'}}{20}\right)^{0.1} \quad \text{in MPa units} \qquad (1)$$

The development length, ℓ_d, of the bonded bars with epoxy adhesive can therefore be evaluated from Eq. (2). It varies between 90 and 97 mm for the 15M bars and is about 62 mm for the 10M bars used for beam B2.

$$\ell_d = \frac{d_b}{4}\frac{f_y}{\tau_b} \qquad (2)$$

Testing procedure and measurements

All beams were tested under three point loading. Fig. 4 shows the experimental setup for a 750 mm deep beam loaded at mid-span. For the 450 mm deep beams, the loading is applied at one-

third of the span only (three point loading). The loading was applied at a rate of 10 mm/h and beam deflections were measured at the loading location. Strain gages (red points in Fig. 3) were used to measure strains in the shear and longitudinal reinforcing bars. LVDTs (Linear Variable Differential Transformers) were installed on the side faces of the beams at mid-depth to measure shear crack width development. A crack comparator was used to measure crack widths. After the tests, concrete core samples were extracted from the beams and some beam sections were cut to examine the anchorage quality of the bonded bars.

For the second test series, after the occurrence of shear failure, the beams were strengthened with steel clamping devices as shown on the right hand side of Fig. 4. This allows the reloading of a beam (40 mm/h) until the failure of the other half of the beam (left hand side of Fig. 4). To distinguish between loading and reloading tests of the same beam, these reloaded beams are identified as beams "R", such as: B4-1R, B5-1R and S1-1R.

Test Results

Table 1 provides a summary of the test results. In this table, the values of the experimental shear force, V_{exp}, (including effects of beam self-weight) and the beam deflection, δ_{exp}, measured at the loading location (see Fig. 4) are given at failure. The applied shear versus δ_{exp} and the critical crack width, *w*, are shown in Fig. 5. Due to failure of the data recording system, no data is available for beam B1-2. Fig. 6 shows the cracking patterns for the half-portion of the beam where the failure occurred. The critical failure cracks are shown with a bold line while the lighter lines show other cracks having smaller crack widths.

Behavior of slab strips

Unstrengthened beams (Beams U1, U2 and U3)

As expected, beam specimens U1, U2 and U3 had only minor diagonal cracking up to the

maximum failure load. Shear failure occurred after the sudden formation of a critical inclined crack and a horizontal splitting crack along the longitudinal reinforcement. These failures occurred suddenly, with little or no warning. The shear strengths of beams U1, U2 and U3 were 324, 291 and 342 kN, respectively. The post-failure resistances were about 100 and 160 kN for beam specimens U1 and U2, respectively. Beams U3 showed almost no post-failure resistance. These tests demonstrate the danger associated with the sudden shear failure mode of concrete thick slab structures without shear reinforcement.

Beam with conventional stirrups (Beam S1)

The main critical shear crack leading to failure was visible on both sides of beam S1 at a shear of about 525 kN and this critical crack progressed slowly during the remaining loading. Beam S1-1 failed at a central deflection of 10.7 mm and a corresponding shear of 726 kN. With a post-failure resistance of 500 kN (decrease of 35%), beam S1-1 exhibited a larger residual shear capacity than the other beams. The reloaded beam test S1-1R was stopped before the shear failure because of the yielding of the steel clamped assemblies used on the other half span. The shear capacity of the beam test S1-1R is therefore higher than 809 kN (see Table 1).

Beams with bonded shear reinforcing bars (Beams B1, B2, B3, B4)

The beams strengthened with drilled-in, bonded shear reinforcing bars exhibited rapid propagation of a wide diagonal crack with a significant decrease of the beam stiffness. For example, for beam B4-1, it can be observed in Fig. 5 that increasing the shear force by 34 kN (508 to 542 kN) resulted in an increase in the central deflection by 1.9 mm (4.6 to 6.5 mm). For this beam, a large crack of width 1.5 mm propagated from the support to the loading location, crossing reinforcing bars R3 and R4 (see Fig. 6 for bar locations). For comparison, the diagonal crack width in beam S1-1 at 525 kN was 0.3 mm and no cracking was visible crossing

reinforcing bars at location R3. For beams B1 and B3, a large critical diagonal crack appeared at 425 and 412 kN, respectively. Thereafter, new diagonal cracks appeared during the loading and the maximum shear capacity of beams B1, B3 and B4 were 471, 498 and 756 kN, respectively. By comparison with the unstrengthened beam specimens U1 and U3, the shear capacity of strengthened beams B1 and B3 increased by about 45% and their deflections at failure increased by 79% and 146%, respectively.

For beam B2-1, no shear crack was visible before the maximum shear capacity of 288 kN was reached at a 6.8 mm deflection. At this load level, a diagonal crack appeared suddenly and the shear force was maintained below the maximum capacity, at a shear of 285 kN, until a sudden loss of the beam capacity, at a deflection of 8.4 mm. For beam B2-2, the shear force was maintained after the propagation of the critical diagonal crack at a shear of 289 kN. The failure of beam B2-2 occurred at a displacement of 9.8 mm and a shear of 315 kN. Compared with the other beams with drilled-in bonded bars, beam B2 showed no additional shear cracking after the propagation of the large diagonal crack. While the strengthening of this beam resulted in an increase in shear capacity of only 4%, the maximum deflection is 25% higher than those measured in the unstrengthened beams U2-1 and U2-2.

As expected, the failure modes of beams B1, B2 and B3, with bonded reinforcing bars, are less brittle: beams B1, B2 and B3 showed signs of their pending failure with large diagonal cracks and higher deformation and post failure capacities than their unstrengthened companion specimens U1, U2 and U3. Likewise, beam B4 showed a similar post failure capacity of 450 kN and a deflection capacity of 12.0 mm as beam S1 with conventional stirrups (500 kN and 10.7 mm).

Beam with overlapped bonded shear reinforcing bars (Beam B5)

Beam B5 with overlapped bonded bars shows more diagonal cracks than the other beams with drilled-in bonded bars. Initially, the progression of most of the diagonal cracks was controlled in the overlapped portion of the shear reinforcing bars. As the load increased, new diagonal cracks appeared in this region. Before the failure, the development of a wide diagonal crack suggested an imminent shear failure. The failure of beam B5-1 is very brittle and the concrete crushed in the compression zone at a deflection of 15.6 mm and a shear of 942 kN. The reloaded beam B5-1R (tested after clamping the failed end) may have been weakened by the very brittle failure of the beam B5-1 and the crushing of the compression zone resulting in a lower shear capacity of 823 kN. Therefore, the experimental capacity obtained for the reloaded beam B5-1R was not used for comparison purposes.

Observation of internal cracking

After testing, the beams were dissected to enable inspection of the internal shear cracking and to see the intersection of this cracking with the added shear reinforcing bars. Fig. 7 shows a view of the inside of beam B5-1R that was strengthened with overlapping bars drilled-in from the top and bottom and then bonded with epoxy. The gaps between the bottom end of bar R2t and the top end of bars R3t and R4t indicate that slippage of the bars had occurred due to debonding. This slippage was most apparent at locations where the shear crack resulted in short embedment lengths of the drilled-in bars.

Behavior of shear reinforcing bars

Fig. 8 shows the average of the measured strain in two stirrup legs, ε_{sv}, versus the central deflection of the beams. The yield strain ($\varepsilon_y = f_y / E_s$) of the shear reinforcing bars is shown as a dashed horizontal line. Table 3 shows the embedded lengths and the distance between the strain gage and the main diagonal crack (L_{tc}). For beam S1-1, the values of L_{tc} for stirrups R2, R3 and

R4 are 128, 30 and 133 mm, respectively. The bar embedded length ℓ_e for the drilled-in bars is taken as the shortest length between the main diagonal crack and the bar extremity. The calculated bar development length, determined from Eq. (2), is shown. The maximum stress in the bar layer $f_{sv,calc}$ is determined according to the bond strength determined from Eq. (1) and is limited by the bar yielding strength. A linear stress-strain relationship, given by Eq. (4) is used to determine the experimental bar stress $f_{sv,exp}$. The maximum values are given in Table 3 according to the maximum bar strain shown in Fig. 8.

$$f_{sv,calc} = \frac{4\tau_b \ell_e}{d_b} \leq f_y \quad (3)$$

$$f_{sv,exp} = E_s \varepsilon_{sv} \leq f_y \quad (4)$$

As seen in Fig. 8, strains in the bonded shear reinforcing bars only occurred after the shear cracking load was reached. For beam B5-1 (Fig. 8), the propagation of two diagonal cracks resulted in increased bar strains at a deflection of about 2.5 mm. The first diagonal crack intercepted the bars at location R2b (see Fig. 6) and its propagation stopped, while the second crack crossed the bars at locations R3b, R3t and R4t. Some beams with shear reinforcement failed shortly after the yielding of one set of added reinforcing bars. The force that can be developed in each bar is a function of the bar embedment length defined by the location of the diagonal crack. When the diagonal crack intercepts a reinforcing bar close to one of its ends, the resulting embedded length ℓ_e could be shorter than ℓ_d and therefore debonding would occur without reaching f_y. For example, it can be seen in Table 3 and Fig. 8 that the diagonal crack occurred near the very end of the bar at location R2 of beam B1-1 resulting in a short embedded length and consequently, this bar debonded.

In interpreting the strain readings, it is important to consider the fact that the reinforcing bar

strain will be at its highest at a crack location. Thus, even if $\ell_e \geq \ell_d$, it can be seen in Fig. 8 and Table 3 that some of the measured strains in the shear reinforcing bars were below ε_y. However, it can be expected that these bars had reached their yield strain at crack locations.

The debonding of some bonded bars can also be seen in Fig. 8. For example, the bars at location R2 in beam B1-1 experienced increasing strains until a maximum of 1659 microstrain ($f_{sv,exp}$ = 332 MPa) at δ_{exp} = 9.9 mm. This was followed by decreasing strains until 652 microstrain ($f_{sv,exp}$ = 130 MPa) at the beam failure (δ_{exp} = 13.7 mm). It can be seen in Table 3 that the maximum predicted bar stress $f_{sv,calc}$ of 242 MPa from Eq. (3) underestimates the experimental value of 332 MPa.

For beam S1-1 with conventional stirrups, the bars at locations R2 and R3 reached their yield strength at a central deflection of 5.7 mm. This is followed by a large increase in the strain of the bars at location R4, reaching a maximum strain 2040 microstrain (408 MPa) at a deflection of 9.9 mm. While the strain gages on the bar at location R4 showed strains below the yield strain, it is possible that this reinforcement yielded at the crack location. For this case, L_{tc} =133 mm and hence these bars may have reached f_y. Compared with beam B4, the conventional stirrup legs in beam S1 are well anchored at both extremities. They cannot slip like the drilled-in bonded bars and therefore, they offer better control of the diagonal cracking. Thus, if the diagonal crack crosses a stirrup near the extremities of the stirrup legs, they are still capable of developing their yield capacity.

Comparison with strength predictions and discussion

The predicted shear capacity V_{calc} was determined at a distance d_v from the edge of the loading plate. The shear design provisions of the Canadian Standards Association (CSA) standard A23.3

(CSA 2014b), the Canadian Highway Bridge Design Code S6 (CSA 2014a) and the AASHTO specifications (AASHTO 2012) are based on the Modified Compression Field Theory (Collins et al. 1996; Bentz and Collins 2004). These requirements define the nominal shear strength attributed to the concrete, V_c, and the shear resistance provided by the shear reinforcement, V_s. The equations from CSA standard A23.3 (CSA 2014b), expressed in SI units, are given below for the nominal shear resistance (i.e., material resistance factors $\phi_c = \phi_s = 1$).

$$V_c = \beta \sqrt{f_c'}\, b_w\, d_v \quad \text{in MPa units} \tag{5}$$

$$\beta = \left(\frac{0.4}{1+1500\varepsilon_x} \right) \left(\frac{1300}{1000 + s_{ze}} \right) \quad \text{mm} \tag{6}$$

$$V_s = A_v\, f_y \frac{d_v \cot\theta}{s_v} \tag{7}$$

Where A_v is the area of transverse reinforcement within a distance s_v and β is the ability of the diagonally cracked concrete to resist shear by tension stiffening and aggregate interlock (Eq. (6)). It is a function of the longitudinal strain, ε_x, at mid-depth of the beam and the equivalent horizontal crack spacing, s_{ze}. For concrete members without transverse reinforcement, $s_{ze} = 35 d_v / \left(16 + a_g\right)$ (mm units). For members containing at least the minimum amount of transverse reinforcement, the equivalent crack spacing parameter s_{ze} is taken as 300 mm (12 in). This minimum amount of transverse reinforcement is determined from Eq. (8), where C = 0.060 for both the CSA S6 code (2014a) and the CSA standard A23.3 (2014b), while C = 0.083, in MPa units for AASHTO specifications (2012).

$$A_v \geq C \frac{\sqrt{f_c'}}{f_y} s_v\, b_w \tag{8}$$

The angle of principal compression in the concrete, θ, with respect to the longitudinal member axis can be used to determine the number of effective transverse reinforcing bars, n_v, resisting shear.

$$n_v = \frac{d_v \cot\theta}{s_v} \tag{9}$$

Unstrengthened beams (Beams U1, U2 and U3)

The calculated shear strength V_{calc} and the experimental shear capacity V_{exp} are given in Table 1. The concrete nominal shear stress at failure ($v_c = V_{exp}/(b_w d_v)$) shows the size effect phenomenon for beams without shear reinforcement. With an effective shear depth, d_v, of 333 mm and 359 mm respectively, beams U1 and U2 experienced a shear stress at failure of 1.59 MPa and 1.33 MPa, respectively, whereas the shear stress at failure of the deepest beam specimens U3 (d_v = 629 mm) failed at a lower shear stress of 0.89 MPa. A good correlation between experimental results and calculated values is achieved with the calculated shear capacity, V_{calc}, for the beams without shear reinforcement being close to V_{exp} (average V_{calc}/V_{exp} = 1.00).

Beam with conventional stirrups (Beam S1)

For both tests on the beams S1-1 (tests S1 for the first loading and S1-1R for the reloading) with stirrups, the predictions are very close to the experimental shear capacities. The average ratio V_{calc}/V_{exp} is 1.05 while the predicted amount of shear reinforcing bars crossed by the diagonal crack n_v is 2.35. These results are in good agreement with the cracking patterns shown in Fig. 6, where the main diagonal crack crossed 3 and 2 bar locations for beams S1-1 and S1-1R, respectively.

Beams with bonded shear reinforcing bars (Beams B1, B2, B3 and B4)

For the beam specimens with epoxy bonded shear reinforcing bars, the predicted shear strengths provided by the bonded shear reinforcing bars are determined from Eq. (7). The experimental cracking patterns showed that the main diagonal crack crossed 2 reinforcing bar locations for beams B2, B3 and B4-1 and 3 locations for beams B1 and B4-1R. Comparing these observations with the values of n_v indicates reasonable predictions of the amount of transverse reinforcement resisting shear. However, with the assumption that the added bars yield, the shear capacities of beams B1, B2 and B3 are overestimated (V_{calc}/V_{exp} = 1.28, 1.42 and 1.41, respectively) while for beam B4 V_{calc}/V_{exp} = 1.07.

Previous measurements showed that bonded bars can fail by debonding before reaching f_y when $\ell_e < \ell_d$ and hence some adjustments are necessary to account for this important effect. As shown in Table 3, all the bonded shear reinforcing bars of beams B4 were able to fully develop their yield strength and therefore, beam B4-1 and B4-1R had a similar behavior to the beam with stirrups and the predicted shear capacity is close to the experimental shear capacity. For beams B1, B2 and B3, a number of bonded bars have partially contributed to the shear capacity due to the fact that a crack crossing a bar within ℓ_d may lead to the debonding of the bar. As illustrated in Fig. 9, the length ℓ_y along a bar where a crossing diagonal crack would allow the development of f_y in the bar can be defined as:

$$\ell_y = \ell_{bar} - 2\ell_d \qquad (10)$$

Where ℓ_{bar} is the bar length and ℓ_d is the bar development length defined by Eq. (2). A diagonal crack is more likely to cross within ℓ_y for small spacings and for long bonded bars. The bar

efficiency ratio in shear η can be defined as follows:

$$\eta = \frac{\ell_y}{d_v} \quad (11)$$

By comparing beams with similar bar development lengths, the bars used for beam B1 and B2 (ℓ_{bar} = 345 mm) are shorter than the bars used for beams B3 (ℓ_{bar} = 645 mm) and B4 (ℓ_{bar} = 660 mm). According to the ℓ_d values presented in Table 3, the bar efficiency ratio η of these beams are 0.45, 0.64, 0.72 and 0.77, respectively. The longer bars used for beams B3 and B4 are therefore more efficient than the bars used for beams B1 and B2.

A small shear reinforcement spacing ratio $k_v = s_v / d_v$ also enables the diagonal crack to cross a larger number of shear reinforcing bars within the yielding length, ℓ_y. For beams B1, B2 and B3, the s_v / d_v values were close to the maximum allowed by standards (0.75 for the S6 code (CSA 2014a) and 0.80 for AASHTO (2012)). Consequently, the main shear cracks intercepted two bar locations near their extremities. However, for beam B4, the smaller ratio k_v of 0.61 allowed the main diagonal crack to cross two bar locations within ℓ_y, with one being intercepted at its mid-height.

Beam with overlapped bonded shear reinforcing bars (Beam B5)

For the shear capacity of beam B5, the overlapped area of shear reinforcing bars is neglected ($A_v = 400$ mm²). The experimental cracking patterns showed that the main diagonal crack crossed 2 reinforcing bar locations, which is similar to the prediction of n_v = 2.35. However, the prediction underestimates the shear capacity for beam B5-1 (V_{calc} / V_{exp} = 0.85). This underestimation can be explained by the overlapping of the bonded bars. The lap length of 300 mm is longer than twice the development length ($2\ell_d$ =182 mm in the epoxy-filled hole). The bar

efficiency ratio η is 1.03 for each pair of overlapped bars and hence the effective bar capacity is higher than $A_v f_y$. As shown in Table 3 for beam B5-1, the yield force of bars R3b was fully developed while the bars R3t reached a maximum stress of 192 MPa ($0.426A_v f_y$) (Table 3). Thus, the two bars R3t and R3b are able to carry a total of 256 kN ($1.426A_v f_y$) instead of 179 kN ($A_v f_y$) assuming $A_v = 400$ mm². In addition, beam B5 has shown a larger number of diagonal cracks in the overlapped bar region than the other beams. The reduction of the crack spacing in the lapped region would likely increase V_c for beam B5.

Maximum spacing of added bonded bars

The experimental results of the beams with added bonded shear reinforcing bars have shown that the maximum bar spacing needs to be smaller than that required in current codes for stirrups. According to current codes (CSA S6 (2014a), CSA A23.3 (2014b) and AASHTO (2012)), stirrups shall be spaced so that every line inclined at an angle θ to the axis of the member and extending toward the reaction from mid-depth to the member longitudinal flexural tension reinforcement shall be crossed by at least one line of effective shear reinforcement. Over the full shear depth, d_v, of the beam, a minimum of two stirrups intercepting the inclined compression field are therefore required. This enables the development of the compression field between two transverse bars carrying tension. The maximum spacing ratio $k_{v,max}$ and the maximum spacing $s_{v,max}$ of transverse reinforcement can therefore be determined as follow:

$$k_{v,max} = \frac{s_{v,max}}{d_v} = \frac{1}{2\tan\theta} \quad (12)$$

For example, for an angle θ of 34°, $k_{v,max}$ = 0.75 as defined by the Canadian Highway Bridge Design Code S6 (CSA 2014a). For bonded bars, the location of the crack determines the bar

embedded length and the bar capacity. For a diagonal crack crossing within the bar yielding length ℓ_y, the transverse reinforcement can reach its yield strength. For cracks crossing within length ℓ_d, partial contribution of the bar is expected. By assuming a constant bond strength along the development length of the bars, the tensile stress f_{sv} that can be developed in the transverse bonded reinforcement can be determined by Eq. (13), where y is the smallest distance measured from the bar extremity (see Fig. 9).

$$f_{sv} = \frac{4\tau_b y}{d_b} \leq f_y \tag{13}$$

The resulting tensile stress distribution in the bonded bars is illustrated in Fig. 9. To meet the maximum spacing requirement, this figure shows how the bonded bars can develop $A_v f_y$ in both lower and upper parts of the beam. The maximum spacing of transverse bonded reinforcement can therefore be determined by Eq. (14).

$$s_{v,max} = k_{v,max}\ell_y \leq k_{v,max}\, d_v \tag{14}$$

Note that using $k_{v,max}\ell_y < s_v < k_{v,max}\ell_{bar}$ results in partial development of the vertical bars. By taking into account the efficiency ratio η from Eq. (11), the maximum spacing ratio of bonded transverse reinforcement can be rewritten as:

$$\frac{s_{v,max}}{d_v} = \eta k_{v,max} \tag{15}$$

Where η is defined by Eq.(11) and is not greater than 1. Because ℓ_d is a constant for a given bonded bar, its efficiency ratio increases as the depth of the slab increases. For shallower slabs, it would be required to use mechanical anchorages at the extremities of the added bars to avoid debonding, or to use inclined bonded bars to increase their embedded length.

From Eq. (15) and $k_v = s_v/\ell_y$, k_v = 1.60, 1.18, 1.04, 0.79 and 0.61 for beams B1, B2, B3, B4 and B5 respectively. Beams B4 and B5 are the only ones meeting the standards requirement ($k_{v,max}$ = 0.75 and 0.80 for the CSA S6 code (2014a) and AASHTO specifications (2012), respectively) while, the transverse bar spacing of the other beams enables partial development of the bonded bars ($k_{v,max}\ell_y < s_v < k_{v,max}\ell_{bar}$). Consequently, the responses of beams B4 and B5 were similar to the beam with stirrups while the shear capacities of the other beams were lower than the ones predicted based on specifications for members with conventional stirrups.

Conclusions

Experiments were carried out on thick concrete slab strips (beams) to evaluate the efficiency of different shear strengthening techniques. The shear capacities were compared to the predictions using current design provisions for elements with or without conventional transverse reinforcements (stirrups). The experimental results showed that:

1. The strengthening techniques resulted in increased shear and deflection capacities compared to beams without shear reinforcement.
2. The beams with added epoxy-bonded bars experienced a rapid propagation of the critical diagonal crack. This resulted in a decrease of stiffness compared with the beams reinforced with conventional stirrups.
3. Short embedded bonded bars ($\ell_e < \ell_d$) failed by debonding at the ends of the bars before reaching f_y and hence adjustments are needed to accurately predict the strength by using current code provisions that assume yielding of the transverse reinforcement.
4. Closely spaced longer bonded bars are more likely to result in yielding of the added epoxy-bonded bars. In such cases, beams exhibit a similar behavior to beams with

stirrups and the predictions using current code provisions accurately predict the shear strength.

5. For added epoxy bonded bars, the maximum spacing required by the current codes for conventional stirrups can result in an overestimation of the shear capacity of up to 48%. Therefore, a maximum spacing requirement for transverse bonded bars has been proposed.
6. The predicted shear capacities using current code provisions for the beams respecting the proposed maximum spacing requirement of the transverse bonded reinforcement (Eq. (15)) agree well with the experimental results.

Acknowledgments

The research reported in this paper was made possible by funding from the Natural Sciences and Engineering Research Council of Canada (NSERC, CREATE-INFRA) and the "Fonds de Recherche du Québec – Nature et Technologies" (FRQNT). The authors also acknowledge the contributions of Philippe Provencher and Benoit Cusson who performed the beam tests. The experiments were carried out in the structures laboratory at Université Laval.

406 **Notation**

407 The following symbols are used in this paper:

408 A_s = area of longitudinal reinforcement on the flexural tension side;

409 A_v = area of shear reinforcement within a distance s_v;

410 b_w = beam web width;

411 d = effective depth to the main tension reinforcement;

412 d_b = reinforcing bar diameter;

413 d_v = effective shear depth, taken as the greater of 0.9d and 0.72h;

414 E_s = modulus of elasticity of steel;

415 $f_c^{'}$ = concrete cylinder compressive strength;

416 f_{sv} = stress in transverse reinforcement;

417 f_y = yield strength of reinforcement;

418 k_v = spacing ratio of transverse reinforcement;

419 ℓ_{bar} = length of added shear reinforcing bar;

420 ℓ_d = bar tension development length;

421 ℓ_e = bar embedded length;

422 ℓ_y = bar yielding length, equal to $\ell_{bar} - 2\ell_d$;

423 n_v = number of effective transverse reinforcing bars;

424 s_v = spacing of transverse reinforcement taken along the member longitudinal axis;

425 s_{ze} = equivalent longitudinal crack spacing;

426 V_c = shear resistance attributed to the concrete;

427 V_s = shear resistance provided by shear reinforcement;

428 β = factor accounting for shear resistance of cracked concrete;

429 γ_c = concrete density (kN/m³);

430 ε_{sv} = strain in transverse reinforcement;

431 ε_x = longitudinal strain at mid-depth of the member;

432 η = bonded bar efficiency ratio in shear;

433 θ = angle of diagonal compressive stresses to the longitudinal axis of the member;

434 ρ = longitudinal reinforcement ratio, equal to $A_s / b_w d$ for a rectangular beam; and

435 τ_b = bond strength of the adhesive (MPa).

436

References

Adhikary, B. B., and Mutsuyoshi, H. (2006). "Shear strengthening of reinforced concrete beams using various techniques." *Constr. Build. Mater.*, 20(6), 366-373.

American Association of State Highway and Transportation Officials (AASHTO). (2012). "AASHTO-LRFD bridge design specifications." Washington, D.C.

Bentz, E.C. and Collins, M.P., "Development of the 2004 CSA A23.3 Shear provisions for reinforced concrete," *Can. J. Civ. Eng.*, 33(5), 521-534.

Canadian Standards Association (CSA). (2014a). "Canadian highway bridge design code." *CSA S6-14*, Mississauga, ON, Canada.

Canadian Standards Association (CSA). (2014b). "Design of concrete structures." *CSA A23.3-14*, Mississauga, ON, Canada.

Collins, M. P., Bentz, E. C., and Sherwood, E. G. (2008). "Where is shear reinforcement required? Review of research results and design procedures." *ACI Struct. J.*, 105(5), 590-599.

Collins, M.P., Mitchell, D., Adebar, P. and Vecchio, F.J. (1996), "A general shear design method", *ACI Struct. J.*, 93 (1), 36-45.

De Lorenzis, L., and Nanni, A. (2001). "Shear strengthening of reinforced concrete beams with near-surface mounted fiber-reinforced polymer rods." *ACI Struct. J.*, 98(1), 60-68.

Dias, S. J. E., and Barros, J. A. O. (2008). "Shear strengthening of T cross section reinforced concrete beams by near-surface mounted technique." *J. Compos. Constr.*, 10.1061/(ASCE) 1090-0268. (2008)12:3(300).

European Technical Approval (ETA). (2013). "Injection system hilti HIT-RE 500." *ETA-04/0027*, Deutsches Institut für Bautechnik, Berlin, Germany.

Fernández Ruiz, M., Muttoni, A., and Kunz, J. (2010). "Strengthening of flat slabs against

460 punching shear using post-installed shear reinforcement." *ACI Struct. J.*, 107(4), 434-442.
461 Godat, A., Qu, Z., Lu, X. Z., Labossière, P., Ye, L. P., and Neale, K.W. (2010). "Size effects for
462 reinforced concrete beams strengthened in shear with CFRP strips." *J. Compos. Const.*,
463 10.1061/(ASCE)CC.1943-5614.0000072.
464 Johnson, P. M., Couture, A., and Nicolet, R. (2007). "Commission of inquiry into the collapse of
465 a portion of the de la Concorde overpass." Library and National Archives of Quebec.
466 ⟨http://www.cevc.gouv.qc.ca/UserFiles/File/Rapport/report_eng.pdf⟩ (Jan. 2015).
467 Mitchell, D., Marchand, J., Croteau, P., and Cook, W. D. (2011). "Concorde overpass collapse:
468 structural aspects." *J. Perform. Constr. Facil.,* 10.1061/(ASCE)CF.1943-5509.0000183.
469 Teng, J. G., Chen, G. M., Chen, J. F., Rosenboom, O. A., and Lam, L. (2009). "Behavior of RC
470 beams shear strengthened with bonded or unbonded FRP wraps." *J. Compos. Const.*,
471 10.1061/(ASCE) CC.1943-5614.0000040.

Table 1. Main properties of tested specimens and comparison to the predicted shear capacities.

Beam designation		Strengthening technique	h mm	d mm	ρ %	d_v mm	A_v mm^2	s_v mm	s_v/d_v	γ_c kN/m^3	f_c MPa	V_{exp} kN	δ_{exp} mm	V_c kN	n_v	V_s	V_{calc} kN	V_{calc}/V_{exp}
Strengthened slabs																		
B1	1	Bonded	450	370	3.10	333	400	240	0.72	22.3	31.7	**471**	13.7	212	2.03	390	**602**	1.28
	2									22.3	33.5	-	-	217	2.03	389	**606**	-
B2	1	Bonded	450	399	2.05	359	200	260	0.72	22.5	34.3	**288**	8.4	248	2.05	179	**426**	1.48
	2									22.6	35.5	**315**	9.8	251	2.05	179	**429**	1.36
B3	1	Bonded	750	699	1.17	629	400	470	0.75	22.7	34.0	**491**	12.3	349	1.82	350	**699**	1.42
	2									22.4	37.2	**505**	11.4	361	1.82	349	**710**	1.40
B4	1	Bonded	750	694	1.65	625	400	380	0.61	22.6	34.5	**743**	12.0	389	2.34	420	**809**	1.09
	1R											**769**	14.4	389	2.34	420	**809**	1.05
B5	1	Overlapped	750	694	1.65	625	400	380	0.61	22.6	32.6	**942**	15.6	380	2.35	421	**801**	0.85
	1R	Bonded										**823**	26.3	380	2.35	421	**801**	0.97
S1	1	Stirrups	750	694	1.65	625	400	380	0.61	22.2	33.3	**726**	10.7	383	2.35	421	**804**	1.11
	1R											**809**	27.1	383	2.35	421	**804**	0.99
																Average		1.22
																CoV		0.17
Unstrengthened slabs																		
U1	1	none	450	370	3.10	333	-	-	-	22.3	31.1	**324**	7.6	285	-	-	**285**	0.88
	2									22.3	33.7	**324**	7.7	293			**293**	0.90
U2	1	none	450	399	2.05	359	-	-	-	22.5	34.9	**278**	6.9	287	-	-	**287**	1.03
	2									22.6	35.7	**304**	7.7	289			**289**	0.95
U3	1	none	750	699	1.17	629	-	-	-	22.4	35.8	**343**	5.0	389	-	-	**389**	1.13
	2									22.7	33.2	**341**	4.6	379			**379**	1.11
																Average		1.00
																CoV		0.11

Note: beams U1, U2, B1 and B2 are loaded at one-third span, while other beams are loaded at mid-span. To distinguish between loading and reloading tests of the same beam, reloaded beams are identified "R". For all beams, width b_w = 610 mm

[a]This beam did not experience shear failure. The capacity was limited by the steel clamped assemblies used to strengthen beam S1-1

Table 2. Steel reinforcing bars properties

Test Series	Bar Designation	d_b (mm)	A_b (mm²)	f_y (MPa)	f_u (MPa)
1st	10M	11.3	100	436	632
	15M	16.0	200	480	690
	25M	25.2	500	468	660
2nd	15M	16.0	200	448	633
	30M	29.9	700	508	668

Table 3. Bonded bars embedded length and bar stress

Beam		Bars	ℓ_e (mm)	ℓ_d (mm)	L_{tc} (mm)	$f_{sv,calc}$ [b] (MPa)	$f_{sv,exp}$ [c] (MPa)
B1	1	R2	50	97.7	4	248	332
		R3	114		42	480	480
		R4	84		30	410	180
	1R	R2	10	97.2	62	51	N/A
		R3	153		20	480	N/A
		R4	85		16	420	N/A
B2	1	R3	93	62.4	20	436	436
		R4	26		0 [a]	178	272
	1R	R3	139	62.2	31	436	436
		R4	45		28	315	270
B3	1	R2	88	97.1	42 [a]	433	378
		R3	119		15	480	480
	2	R2	27	96.2	95	136	144
		R3	119		11	480	480
B4	1	R3	308	90.5	88	448	448
		R4	128		92 [a]	448	374
	1R	R2	135	90.5	146	448	431
		R3	327		107	448	448
		R4	124		96	448	61
B5	1	R3b	129	91.0	195 [a]	448	448
		R3t	39		146	192	N/A
		R4t	172		17	448	448
	1R	R2b	196	91.0	194	448	448
		R2t	35		110	171	N/A
		R3b	16		169	77	N/A
		R3t	202		21	448	448
		R4t	111		75	448	439

[a] Several cracks cross the transverse reinforcing bar. The bar embedded length and the relative distance to the strain gage are not measured with the same crack.
[b] Determined with Eq. 3.
[c] Determined with Eq. 4 and the maximum measured bar strain in Fig. 8.

Fig 1a

Click here to download Figure Fig 1a.pdf

Fig 1b

Click here to download Figure Fig 1b.pdf

Fig 2a

Click here to download Figure Fig 2a.pdf

Fig 2b

Click here to download Figure Fig 2b.pdf

Fig 3a

Click here to download Figure Fig 3a.pdf

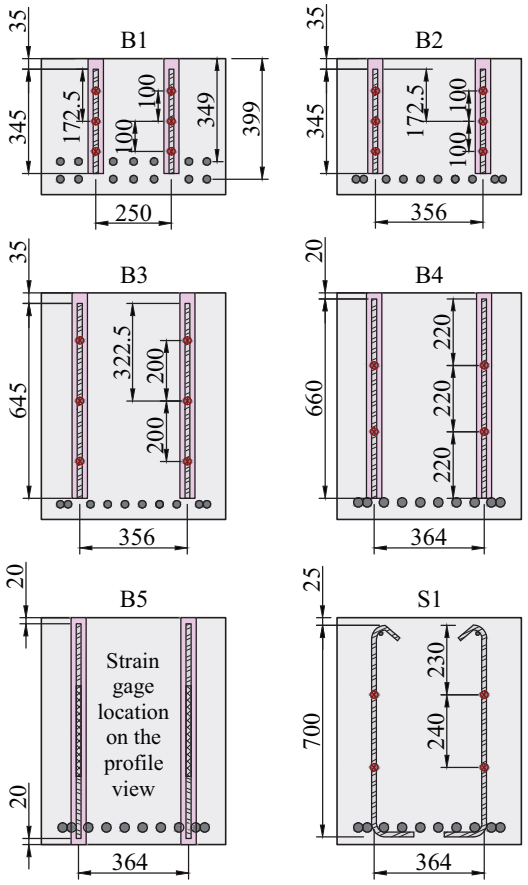

Fig 3b

Click here to download Figure Fig 3b.pdf

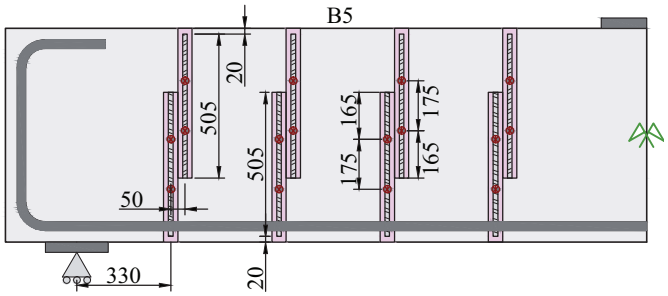

Fig 4

Click here to download Figure Fig 4.pdf

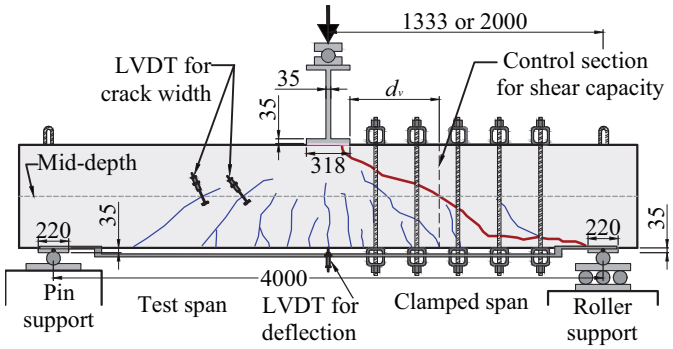

Fig 5

Click here to download Figure Fig 5.pdf

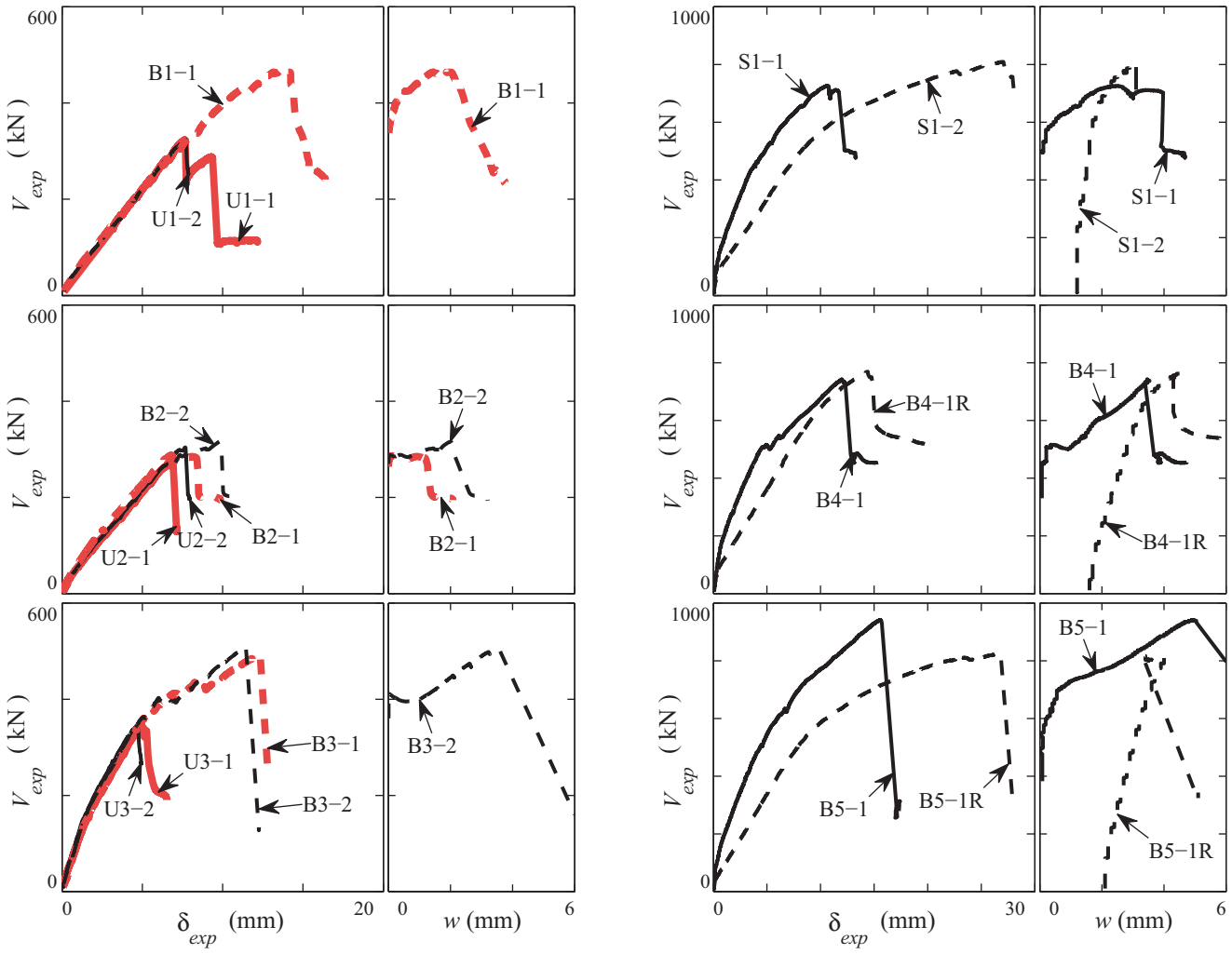

Fig 6

Click here to download Figure Fig 6.pdf

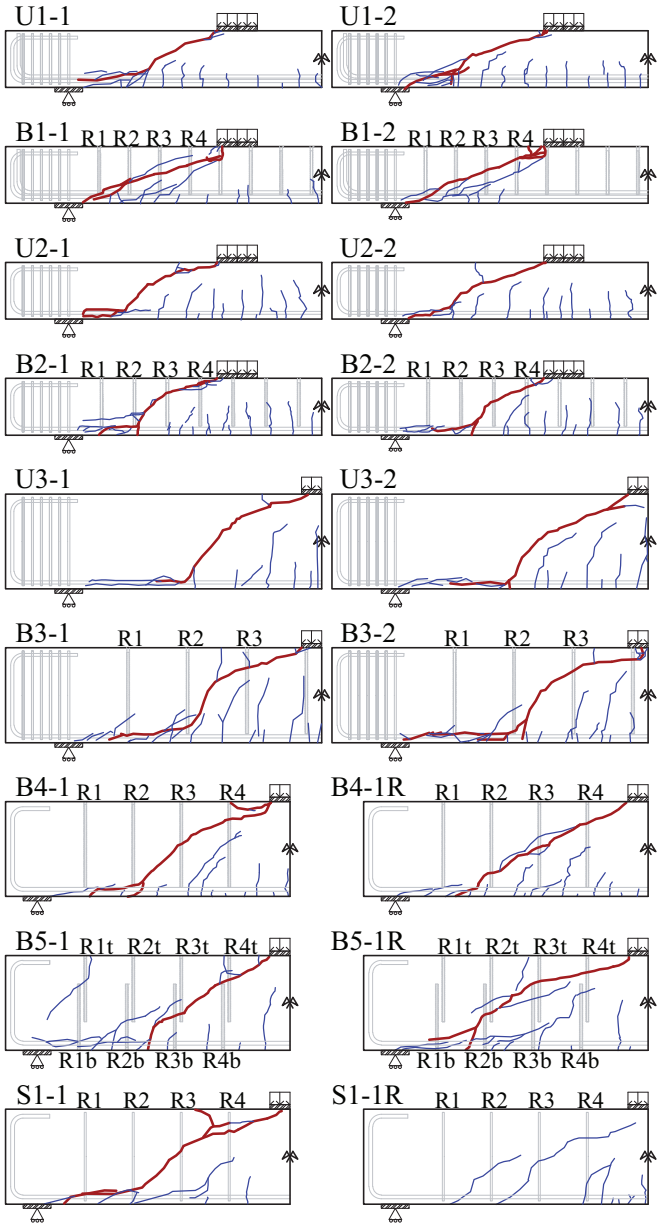

Fig 7a

Click here to download Figure Fig 7a.pdf

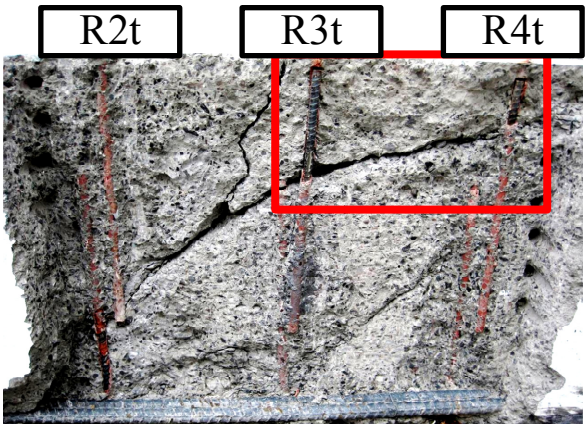

Fig 7b

Click here to download Figure Fig 7b.pdf

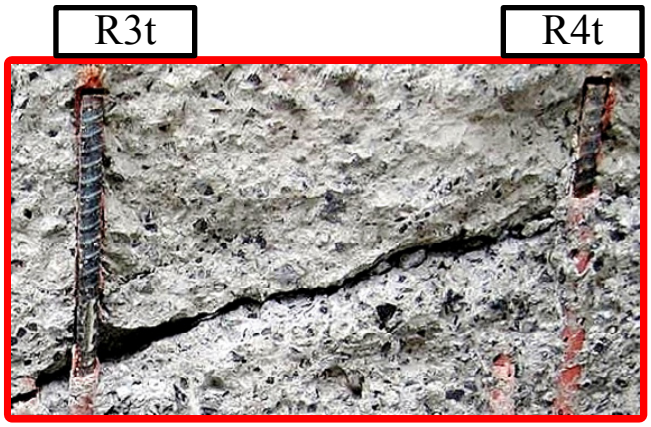

Fig 8

Click here to download Figure Fig 8.pdf

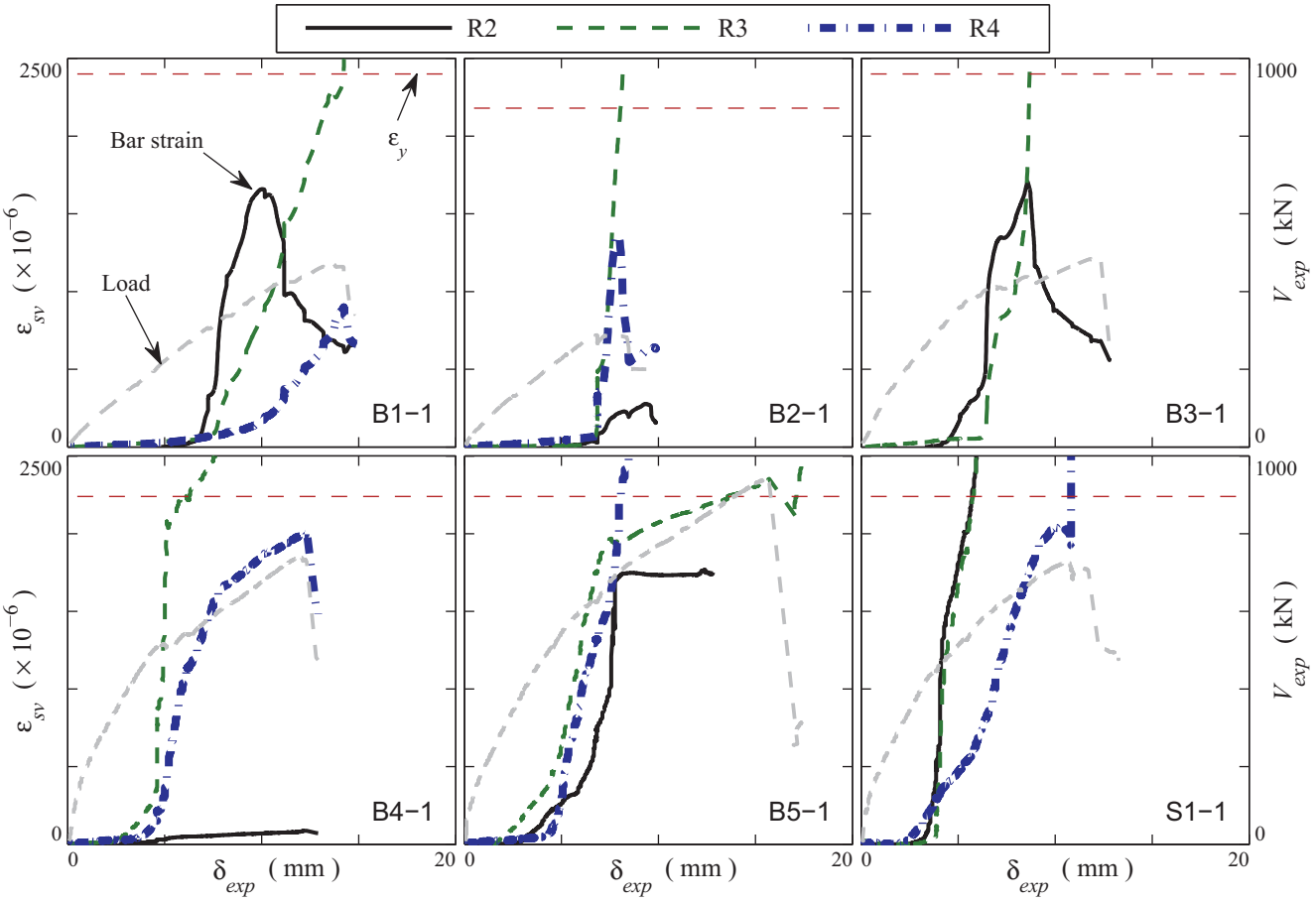

Fig 9

Click here to download Figure Fig 9.pdf

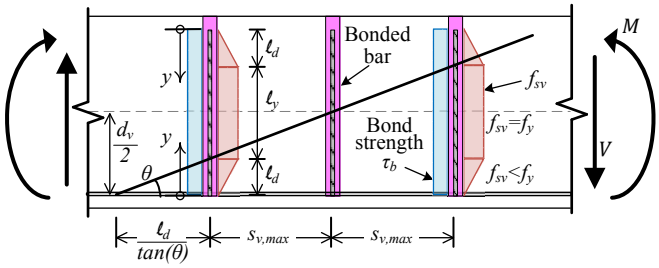

Figure caption list

Fig. 1. Partial collapse of south portion of Concorde Overpass due to shear failure of thick slab (a) Aerial view of south portion (with permission Johnson et al. 2007) and (b) Shear failure of thick slab that started near southeast corner (image by D. Mitchell)

Fig. 2. Installation of the epoxy bonded bars (a) from the top beam surface and (b) from the bottom beam surface (image by J. Bastien)

Fig. 3. (a) Tested strengthened slab slices specimens (b) Profile view of beam B5 (dimensions in mm)

Fig. 4. Experimental setup for reloading (R) stage (dimensions in mm)

Fig. 5. Load V_{exp} and critical shear crack width w vs beam deflection curves δ_{exp}

Fig. 6. Cracking pattern of tested beam

Fig. 7. Profile cut section of beam test B5-1R (a) Overall view of internal shear crack (b) Close-up of shear failure crack (image by J. Bastien)

Fig. 8. Strain of shear reinforcing bars near the main shear crack and applied load vs beam deflection (for beam B5-1, bars R2, R3 and R4 refer to R2b, R3b and R4t)

Fig. 9. Maximum bar spacing for beam with bonded shear reinforcing bars